JOC*Article*

Reaction Pathways and Free Energy Barriers for Alkaline Hydrolysis of Insecticide 2-Trimethylammonioethyl Methylphosphonofluoridate and Related Organophosphorus Compounds: Electrostatic and Steric Effects

Ying Xiong and Chang-Guo Zhan*

Key Laboratory of Pesticide & Chemical Biology of the Ministry of Education, College of Chemistry, Central China Normal University, Wuhan 430079, P. R. China, and Department of Pharmaceutical Sciences, College of Pharmacy, University of Kentucky, 725 Rose Street, Lexington, Kentucky 40536

zhan@uky.edu

Received July 20, 2004

Reaction pathways and free energy barriers for alkaline hydrolysis of the highly neurotoxic insecticide 2-trimethylammonioethyl methylphosphonofluoridate and related organophosphorus compounds were studied by performing first-principles electronic structure calculations on representative methylphosphonofluoridates, $(RO)CH_3P(O)F$, in which R = $CH_2CH_2N^+(CH_3)_3$, CH_3, $CH_2CH_2C(CH_3)_3$, $CH_2CH_2CH(CH_3)_2$, $CH(CH_3)CH_2N^+(CH_3)_3$, and $CH(CH_3)CH_2N(CH_3)_2$. The dominant reaction pathway was found to be associated with a transition state in which the attacking nucleophile OH^- and the leaving group F^- are positioned on opposite sides of the plane formed by the three remaining atoms attached to the phosphorus in order to minimize the electrostatic repulsion between these two groups. The free energy barriers calculated for the rate-determining step of the dominant pathway are 12.5 kcal/mol when R = $CH_2CH_2N^+(CH_3)_3$, 15.5 kcal/mol when R = CH_3, 17.9 kcal/mol when R = $CH_2CH_2C(CH_3)_3$, 16.5 kcal/mol when R = $CH_2CH_2CH(CH_3)_2$, 13.4 kcal/mol when R = $CH(CH_3)CH_2N^+(CH_3)_3$, and 18.7 kcal/mol when R = $CH(CH_3)CH_2N(CH_3)_2$. The calculated free energy barriers are in good agreement with available experimentally derived activation free energies, i.e. 14.7 kcal/mol when R = CH_3, 13.4 kcal/mol when R = $CH_2CH_2N^+(CH_3)_3$, and 13.9 kcal/mol when R = $CH(CH_3)CH_2N^+(CH_3)_3$. A detailed analysis of the calculated energetic results and available experimental data suggests that the net charge of the molecule (M) being hydrolyzed is a prominent factor affecting the free energy barrier (ΔG) for the alkaline hydrolysis of phosphodiesters, phosphonofluoridates, and related organophosphorus compounds. The electrostatic interactions between the attacking nucleophile OH^- and the molecule M being hydrolyzed favor such an order of the free energy barrier: $\Delta G(M^+ + OH^-) < \Delta G(M^0 + OH^-) < \Delta G(M^- + OH^-)$, where M^+, M^0, and M^- represent the cationic, neutral, and anionic molecules, respectively. The change of the substituent R in $(RO)CH_3P(O)F$ from CH_3 to $CH_2CH_2N^+(CH_3)_3$ is associated with both the electrostatic and steric effects on the free energy barrier, but the electrostatic effect dominates the substituent shift of the free energy barrier. This helps to better understand why the alkaline hydrolysis of $(RO)CH_3P(O)F$ with R = $CH_2CH_2N^+(CH_3)_3$ and $CH(CH_3)CH_2N^+(CH_3)_3$ is significantly faster than that with R = CH_3. The effect of electrostatic interaction also helps to understand why the rate constants for the alkaline hydrolysis of phosphodiesters, such as intramolecular second messenger adenosine 3′,5′-phosphate (cAMP), are generally smaller than those for the alkaline hydrolysis of the phosphonofluoridates and related phosphotriesters.

Introduction

Phosphorus has a broad role in living systems, and hydrolysis of phosphate esters and their structural variants in solution and in enzymes is one of the most fundamental types of chemical and biochemical reactions.[1] A phosphonofluoridate, (RO)R′P(O)F, may be considered to be a structural variant of a phosphotriester in which two of the three OR groups are replaced by a F atom and a R′ group. A variety of phosphonofluoridates have been used either as agriculture insecticides,[2] such as 2-trimethylammonioethyl methylphosphonofluoridate in which R′ = CH_3 and R = $CH_2CH_2N^+(CH_3)_3$, or as chemical warfare nerve gases, such as *O*-isopropyl methylphosphonofluoridate (sarin) and *O*-pinacolyl methylphosphonofluoridate (soman).[3] These organophosphorus compounds are extremely potent, irreversible inhibitors

* Address correspondence to this author at the University of Kentucky.

(1) Westheimer, F. H. *Science* **1987**, *235*, 1173.

(2) O'Brien, R. D. *Toxic phosphorus esters*: *chemistry*, *metabolism and biological effects*; Academic Press: New York, 1960.

(3) Zheng, F.; Zhan, C.-G.; Ornstein, R. *J. Chem. Soc.*, *Perkin Trans. 2* **2001**, 2355.

10.1021/jo0487597 CCC: $27.50
Published on Web 11/04/2004

of acetylcholinesterase (AChE), a critical enzyme responsible for regulating the concentration of the neurotransmitter acetylcholine (ACh) through AChE-catalyzed hydrolysis of ACh. Exposure to excess levels of these organophosphorus compounds not only has immediate consequences but also has been shown to exert delayed cholinergic toxicity and delayed neurotoxicity.[4] Long-term exposure to low levels of these organophosphorus compounds can produce persistent and additive inhibition of AChE resulting in a delayed neuropathy.[5] So, the phosphonofluoridates are highly neurotoxic to both target and nontarget organisms.

It is interesting to develop an efficient approach to the chemical destruction of these neurotoxic organophosphorus compounds for the purposes of chemical defense and environmental protection.[6−10] However, the extreme toxicity of the compounds makes the experimentations with the actual compounds extremely difficult.[11] We are particularly interested in understanding the detailed reaction mechanisms for hydrolytic degradation of these neurotoxic organophosphorus compounds through computational studies, because detailed state-of-the-art computational studies could lead to some useful insights that can help to minimize the number of risk experimental tests required to achieve a goal of investigation.

This study is focused on the mechanisms for alkaline hydrolysis of phosphonofluoridates. Experimental rate constants have been known for the alkaline hydrolysis of some phosphonofluoridates.[2] The experimental data collected by O'Brien[2] indicate that methylphosphonofluoridates, $(RO)CH_3P(O)F$, are usually associated with larger rate constants compared to other phosphonofluoridates, and that the insecticide 2-trimethylammonioethyl methylphosphonofluoridate has the largest rate constant (935 M^{-1} s^{-1}). The substituent shifts of the rate constant for the $(RO)R'P(O)F$ hydrolysis are remarkable and the substituent shifts of the rate constant may be attributed, in most of the cases, to the effects of steric hindering of substituents R and R′ to the attack of the nucleophile (HO^-).[2] Consideration of the steric effect suggests that the larger the bulk size of R or R′, the lower the rate constant of the $(RO)R'P(O)F$ hydrolysis, thus explaining the fact that the rate constant of the $(RO)R'P(O)F$ hydrolysis decreases by increasing the size of R or R′ from CH_3 to C_2H_5 to C_3H_7.[2] However, the steric effect alone cannot help to explain why the rate constant (935 M^{-1} s^{-1}) of the hydrolysis of 2-trimethylammonioethyl methylphosphonofluoridate, in which $R' = CH_3$ and $R = CH_2CH_2N^+(CH_3)_3$, is even significantly larger than that (106 M^{-1} s^{-1}) of the hydrolysis of the smallest phosphonofluoridate in which $R' = CH_3$ and $R = CH_3$.[2]

The "abnormal" substituent shift of the rate constant of the $(RO)CH_3P(O)F$ hydrolysis from $R = CH_3$ to $CH_2CH_2N^+(CH_3)_3$ might be associated with the change of the formal charge on R. $(RO)CH_3P(O)F$ is a neutral molecule when $R = CH_3$, but it becomes a cation when $R = CH_2CH_2N^+(CH_3)_3$. A question is how the charged functional group, $CH_2CH_2N^+(CH_3)_3$, contributes to the significant increase of the rate constant of the hydrolysis. Does this charged functional group change the fundamental reaction pathway, change the orientation of the HO^- attack at the P center, or simply stabilize the transition state of the hydrolysis? A recently reported computational study[3] of reaction pathways for a neutral phosphotriester (paraoxon) and its neutral variants indicates that the alkaline hydrolysis of these compounds proceeds with a net inversion of stereochemistry at the phosphorus center, i.e. via a pathway that the attacking nucleophile (OH^-) and the leaving group (e.g. F^- in a variant) are positioned on opposite sides of the plane formed by the three remaining atoms attached to the P atom,[3] but no charged molecule (phosphotriester or its variant) was examined in the reaction coordinate calculations. Is the pathway found for the hydrolysis of the neutral molecules still correct for the positively charged molecule, i.e. $(RO)CH_3P(O)F$ when $R = CH_2CH_2N^+(CH_3)_3$?

To answer these questions, we have performed detailed reaction coordinate calculations on the hydrolysis of the charged phosphonofluoridate, i.e. 2-trimethylammonioethyl methylphosphonofluoridate, in consideration of two competing orientations of the HO^- attack. The corresponding free energy barriers have been evaluated to determine the dominant pathway. In addition, the same computational protocol has also been used to examine the reaction pathways and free energy barriers for the hydrolysis of two neutral methylphosphonofluoridates, i.e. $(RO)CH_3P(O)F$ when $R = CH_3$ and $CH_2CH_2C(CH_3)_3$. A detailed comparison and analysis of the calculated results leads to a deeper understanding of the electrostatic and steric effects on the free energy barriers for alkaline hydrolysis of phosphonofluoridates and related phosphate esters.

Calculation Methods

Geometries of all reactants, transition states, intermediates, and products involved in this study were optimized by using the Hartree−Fock (HF) method with the 6-31+G(d) basis set. Vibrational frequency calculations were carried out to ensure that the optimized geometries are indeed local minima or saddle points on the potential energy surfaces and to determine the zero-point vibrational energies (ZPVE's) and thermal

(4) (a) Abou-Donia, M. B.; Graham, D. G.; Timmons, P. R.; Reichert, B. L. *Neurotoxicology* **1979**, *1*, 425. (b) Ali, F. A. F.; Fukuto, T. R. *J. Toxicol. Environ. Health* **1983**, *12*, 591. (c) Metcalf, R. L. *Neurotoxicology* **1982**, *3*, 269.

(5) Williams, F. M.; Charlton, C.; Deblaquiere, G. E.; Mutch, E.; Kelly, S. S.; Blain, P. G. *Hum. Exp. Toxicol*. **1997**, *16*, 67.

(6) (a) Yang, Y.-C.; Berg, F. J.; Szafraniec, L. L.; Beaudry, W. T.; Bunton, C. A.; Kumar, A. *J. Chem. Soc., Perkin Trans*. **1997**, *2*, 607. (b) Bhattacharya, S.; Snehalatha, K. *J. Org. Chem*. **1997**, *62*, 2198. (c) Toullec, J.; Moukawim, M. *Chem. Commun*. **1996**, 221. (d) Bunton, C. A.; Foroudian, H. J. *Langmuir* **1993**, *9*, 2832. (e) Yang, Y.-C.; Szafraniec, L. L.; Beaudry, W. T.; Bunton, C. A. *J. Org. Chem*. **1993**, *58*, 6964.

(7) (a) Moss, R. A.; Kotchevar, A. T.; Park, B. D.; Scrimin, P. *Langmuir* **1996**, *12*, 2200. (b) Moss, R. A.; Bose, S. *Tetrahedron Lett*. **1997**, *38*, 965. (c) Berg, F. J.; Moss, R. A.; Yang, Y.-C.; Zhang, H. *Langmuir* **1995**, *11*, 411. (d) Moss, R. A.; Bracken, K.; Emge, T. J. *J. Org. Chem*. **1995**, *60*, 7739. (e) Moss, R. A.; Bose, S.; Ragunathan, K. G.; Jayasuriya, N.; Emge, T. J. *Tetrahedron Lett.* **1998**, *39*, 347.

(8) (a) Scrimin, P.; Ghirlanda, G.; Tecilla, P.; Moss, R. A. *Langmuir* **1996**, *12*, 6235. (b) Kimura, E.; Hashimoto, H.; Koike, T. *J. Am. Chem. Soc*. **1996**, *118*, 10963. (c) Weijnen, J. G. J.; Engbersen, J. F. *J. Recl. Trav. Chim*. **1993**, *112*, 351. (d) Gellman, S. H.; Petter, R.; Breslow, R. *J. Am. Chem. Soc*. **1986**, *108*, 2388. (e) Menger, F. M.; Gan, L. H.; Johnson, E.; Durst, H. D. *J. Am. Chem. Soc*. **1987**, *109*, 2800.

(9) (a) Vanhooke, J. L.; Benning, M. W.; Raushel, F. M.; Holden, H. M. *Biochemistry* **1996**, *35*, 6020. (b) Benning, M. W.; Kuo, J. M.; Raushel, F. M.; Holden, H. M. *Biochemistry* **1994**, *33*, 15001.

(10) (a) Weiner, D. P.; Weimann, T.; Wolfe, M. M.; Wentworth, P., Jr.; Janda, K. D. *J. Am. Chem. Soc.* **1997**, *119*, 4088. (b) Lavey, B. J.; Janda, K. D. *J. Org. Chem*. **1996**, *61*, 7633. (c) Rosenblum, J. S.; Lo, L.-C.; Li, T.; Janda, K. D.; Lerner, R. A. *Angew. Chem., Int. Ed. Engl.* **1995**, *34*, 2275.

(11) (a) Bunton, C. A.; Robinson, L. *J. Org. Chem*. **1969**, *34*, 773. (b) Moss, R. A.; Ihara, Y. *J. Org. Chem*. **1983**, *48*, 588.

corrections to the Gibbs free energies. No empirical scaling factor was used to scale the calculated vibrational frequencies because, for the calculated free energy barriers, the ZPVE corrections and the vibrational contributions to the thermal corrections are all very small due to the cancellations. Intrinsic reaction coordinate (IRC)[12] calculations were performed at the HF/6-31+G(d) level to confirm the optimized transition state geometries. The geometries optimized at the HF/6-31+G(d) level were employed to perform the second-order Møller–Plesset (MP2) energy calculations with the 6-31+G(d), 6-31++G(d,p), and 6-311++G(d,p) basis sets.

Previous theoretical studies[13−15] of reaction pathways for alkaline ester hydrolyses indicate that electron correlation effects are not important in the optimizations of molecular geometries and calculations of solvent shifts, but are important in final energy calculations, for studying energy profiles of those organic reactions. With a given basis set, the energy barriers evaluated by performing the MP2 energy calculations with use of the MP2 geometries are all very close to those evaluated by the MP2 calculations by using geometries optimized with the HF and density functional theory (DFT) methods. The energy barriers calculated with the MP2 method are all very close to those calculated with MP4SDQ, QCISD, and QCISD(T) methods,[13] indicating that the MP2 method is sufficiently accurate for recovery of the electron correlation. It should be pointed out that the methodology discussion here is limited to the hydroxide ion-catalyzed hydrolysis reactions.[13−15]

Self-consistent reaction field (SCRF) energy calculations were performed to calculate solvent shifts of the free energy barriers by using the geometries optimized at the HF/6-31+G-(d) level in the gas phase. Florian and Warshel performed a manual geometry search in solution along the corresponding gas-phase intrinsic reaction coordinate for the hydrolysis of monomethyl phosphate and demonstrated that the contributions of the solvent-induced structural changes to the overall energetics are small and can be safely neglected.[16] The same conclusion was also obtained from first-principles computational studies on hydroxide ion-catalyzed hydrolysis of a phosphotriester and its structural variants.[17] The free energy barrier for reaction in aqueous solution was taken as a sum of the free energy change calculated at the MP2/6-31+G(d)//HF/6-31+G(d) level in the gas phase and the corresponding solvent shift determined by the SCRF calculations at the HF/6-31+G(d) level. The SCRF method used in the calculations is a recently developed GAMESS implementation[18] of the surface and volume polarization for electrostatic interactions (SVPE).[19] The SVPE model is also known as the fully polarizable continuum model (FPCM)[20] because it fully accounts for both surface and volume polarization effects in the SCRF calculation. In other SCRF implementations, volume polarization effects are ignored or approximately modeled by modifying the surface polarization charge distribution through a simulation and/or charge renormalization,[21−29] or the solute charge distribution is simply represented by a set of point charges at the solute nuclei.[30,31]

Since the solute cavity surface is defined as a solute electron charge isodensity contour determined self-consistently during the SVPE iteration process, the SVPE results, converged to the exact solution of Poisson's equation with a given numerical tolerance, depend only on the contour value at a given dielectric constant and a certain quantum chemical calculation level.[19a] Our previous computational studies involving SVPE calculations have demonstrated that the SVPE calculations with the 0.002 au contour led to the calculated energy barriers in good agreement with the corresponding experimental data for the hydroxide ion-catalyzed ester hydrolysis reactions.[15,17,32,33] Besides, Bentley recently employed the minimum in the electron density function between pairs of interacting molecules to estimate molecular sizes, and found that the molecular surfaces identified by such a procedure are in excellent agreement with the 0.002 au isodensity contour.[34] So, the 0.002 au contour was used in this study.

The current version[19a] of the SVPE implementation has its own limitations. In particular, the analytic energy derivatives required for geometry optimization and the calculations of the short-range nonelectrostatic interactions have not been implemented yet and the short-range nonelectrostatic interactions have significant contributions to the absolute hydration free energy of a charged species.[35] Nevertheless, for a given chemical reaction step, the short-range nonelectrostatic contributions to the energy change can nearly cancel out and the overall effects of the short-range nonelectrostatic contributions on the free energy barriers are negligible.[17,32,33] Previous computational studies[14,15,17,32,33] demonstrate that, whether the short-range nonelectrostatic interactions are included or not, the first-principles electronic structure calculations with the SVPE method can consistently predict energy barriers and free energy barriers in excellent agreement with the corresponding experimental data for the alkaline hydrolyses of carboxylic acid esters, phosphate esters, and their structural variants.

The SVPE solvation calculations were performed with a local version[19a] of the GAMESS program and all other results

(12) (a) Gonzalez, C.; Schlegel, H. B. *J. Chem. Phys*. **1989**, *90*, 2154. (b) Gonzalez, C.; Schlegel, H. B. *J. Phys. Chem*. **1990**, *94*, 5523.
(13) Zhan, C.-G.; Landry, D. W.; Ornstein, R. L. *J. Am. Chem. Soc.* **2000**, *122*, 1522.
(14) Zhan, C.-G.; Landry, D. W.; Ornstein, R. L. *J. Am. Chem. Soc.* **2000**, *122*, 2621.
(15) Zhan, C.-G.; Landry, D. W.; Ornstein, R. L. *J. Phys. Chem. A* **2000**, *104*, 7672.
(16) Florian, J.; Warshel, A. *J. Phys. Chem. B* **1998**, *102*, 719.
(17) Zheng, F.; Zhan, C.-G.; Ornstein, R. L. *J. Chem. Soc.*, *Perkin Trans. 2* **2001**, 2355.
(18) Schmidt, M. W.; Baldridge, K. K.; Boatz, J. A.; Elbert, S. T.; Gordon, M. S.; Jensen, J. H.; Koseki, S.; Matsunaga, N.; Nguyen, K. A.; Su, S. J.; Windus, T. L.; Dupuis, M.; Montgomery, J. A. *J. Comput. Chem.* **1993**, *14*, 1347.
(19) (a) Zhan, C.-G.; Bentley, J.; Chipman, D. M. *J. Chem. Phys.* **1998**, *108*, 177. (b) Zhan, C.-G.; Chipman, D. M. *J. Chem. Phys.* **1998**, *109*, 10543. (c) Zhan, C.-G.; Chipman, D. M. *J. Chem. Phys.* **1999**, *110*, 1611.
(20) (a) Zhan, C.-G.; Norberto de Souza, O.; Rittenhouse, R.; Ornstein, R. L. *J. Am. Chem. Soc.* **1999**, *121*, 7279. (b) Zhan, C.-G.; Zheng, F. *J. Am. Chem. Soc.* **2001**, *123*, 2835. (c) Zheng, F.; Zhan, C.-G.; Ornstein, R. L. *J. Phys. Chem. B* **2002**, *106*, 717. (d) Zhan, C.-G.; Dixon, D. A.; Sabri, M. I.; Kim, M.-S.; Spencer, P. S. *J. Am. Chem. Soc.* **2002**, *124*, 2744. (e) Dixon, D. A.; Feller, D.; Zhan, C.-G.; Francisco, S. F. *J. Phys. Chem. A* **2002**, *106*, 3191. (f) Dixon, D. A.; Feller, D.; Zhan, C.-G.; Francisco, S. F. *Int. J. Mass Spectrom*. **2003**, *227*, 421. (g) Zhan, C.-G.; Dixon, D. A.; Spencer, P. S. *J. Phys. Chem. B* **2003**, *107*, 2853. (h) Zhan, C.-G.; Dixon, D. A.; Spencer, P. S. *J. Phys. Chem. B* **2004**, *108*, 6098.
(21) Tomasi, J.; Persico, M. *Chem. Rev*. **1994**, *94*, 2027.
(22) Mejias, J. A.; Lago, S. *J. Chem. Phys.* **2000**, *113*, 7306.
(23) Cramer, C. J.; Truhlar, D. G. In *Solvent Effects and Chemical Reactions*; Tapia, O., Bertran, J., Eds.; Kluwer: Dordrecht, The Netherlands, 1996; p 1.
(24) Chipman, D. M. *J. Chem. Phys.* **2000**, *112*, 5558.
(25) Barone, V.; Cossi, M.; Tomasi, J. *J. Chem. Phys.* **1997**, *107*, 3210.
(26) Tomasi, J.; Mennucci, B.; Cances, E. *J. Mol. Struct.* (*THEOCHEM*) **1999**, *464*, 211.
(27) Cancès, E.; Mennucci, B. *J. Chem. Phys.* **2001**, *114*, 4744.
(28) Cossi, M.; Rega, N.; Scalmani, G.; Barone, V. *J. Chem. Phys.* **2001**, *114*, 5691.
(29) Chipman, D. M. *J. Chem. Phys.* **2002**, *116*, 10129.
(30) Tawa, G. J.; Topol, I. A.; Burt, S. K.; Caldwell, R. A.; Rashin, A. A. *J. Chem. Phys.* **1998**, *109*, 4852.
(31) Topol, I. A.; Tawa, G. J.; Burt, S. K.; Rashin, A. A. *J. Chem. Phys.* **1999**, *111*, 10998.
(32) Chen, X.; Zhan, C.-G. *J. Phys. Chem. A* **2004**, *108*, 3789.
(33) Chen, X.; Zhan, C.-G. *J. Phys. Chem. A* **2004**, *108*, 6407.
(34) Bentley, J. *J. Phys. Chem. A* **1998**, *102*, 6043.
(35) (a) Zhan, C.-G.; Dixon, D. A. *J. Phys. Chem. A* **2001**, *105*, 11534. (b) Zhan, C.-G.; Dixon, D. A. *J. Phys. Chem. A* **2002**, *106*, 9737. (c) Zhan, C.-G.; Dixon, D. A. *J. Phys. Chem. A* **2003**, *107*, 4403. (d) Zhan, C.-G.; Dixon, D. A. *J. Phys. Chem. A* **2004**, *108*, 2020.

were obtained with the Gaussian03 program[36] on an HP's Superdome supercomputer, two Linux clusters, and SGI multiprocessors Origin computers.

Results and Discussion

Alkaline Hydrolysis of 2-Trimethylammonioethyl Methylphosphonofluoridate. We first examined the reaction pathway (pathway A) where the attacking nucleophile OH^- and the leaving group F^- are positioned on opposite sides of the plane formed by the three remaining atoms attached to the phosphorus. Geometries of the reactant (Reactant-1), hydrogen-bonded reactant complex (HBR-1A), transition states (TS1-1A and TS2-1A), intermediate (INT-1A), and product (Product-1A) optimized for this pathway are depicted in Figure 1, along with the geometry of the first transition state (TS1-1B) optimized for another reaction pathway (pathway B). Some key geometric parameters are indicated in the figure. Concerning the structural notations used in Figure 1, the number "1" after the dash refers to 2-trimethylammonioethyl methylphosphonofluoridate (molecule #1 calculated in this study), i.e. $(RO)CH_3P(O)F$ when $R = CH_2CH_2N^+(CH_3)_3$. Similarly, the numbers "2" to "6" in Figures 2 and 3 refer to other methylphosphonofluoridates in which $R = CH_3$ (molecule #2), $R = CH_2CH_2C(CH_3)_3$ (molecule #3), $R = CH_2CH_2CH(CH_3)_2$ (molecule #4), $R = CH(CH_3)CH_2N^+(CH_3)_3$ (molecule #5), and $R = CH(CH_3)CH_2N(CH_3)_2$ (molecule #6), respectively.

Previous computational studies[14,15,17] have already demonstrated that hydroxide ion-catalyzed hydrolysis reactions involve formation a stable hydrogen-bonded reactant complex, i.e. a complex of the molecule to be hydrolyzed with a hydroxide ion, in the gas phase before going to the first transition state TS1 of the hydrolysis. However, in aqueous solution the total energy of the separated reactants becomes lower than that of the hydrogen-bonded reactant complex (HBR) for all of the compounds examined. Thus, in aqueous solution the HBR structure is no longer associated with a local minimum on the potential energy surface and the reaction goes directly from the separated reactants to TS1.[14,15,17] The calculated results in the present study confirm this conclusion. So, the energy barrier calculated for the first step of such a reaction in the gas phase should be the energy change from HBR to TS1, whereas the energy barrier calculated for the first step of such a reaction in aqueous solution should be the energy change from the separated reactants to TS1.

As seen in Figure 1, pathway A involves two major reaction steps starting from Reactant-1 + HO^- (in aqueous solution) or a hydrogen-bonded reactant complex HBR-1A (in the gas phase). The first step is the formation of a pentacoordinated phosphorus intermediate, INT-1A, through transition state TS1-1A and the second step is the decomposition of the intermediate to the product (Product-1 + F^-) through transition state TS2-1A. A notable feature of the optimized TS1-1A geometry is associated with four C−H···O hydrogen bonds[37] involving the hydroxide oxygen: three strong C−H···O hydrogen bonds with $CH_2CH_2N^+(CH_3)_3$ and a weak C−H···O hydrogen bond with the CH_3 group on the P atom, as suggested by the optimized H···O internuclear distances in Figure 1. These hydrogen bonds are expected to stabilize the transition state and, thus, lower the free energy barrier for this reaction step. The total $n_O \rightarrow \sigma^*_{C-H}$ delocalization energy associated with the three C−H···O hydrogen bonds with $CH_2CH_2N^+(CH_3)_3$ was calculated to be 30.6 kcal/mol, whereas the total $n_O \rightarrow \sigma^*_{C-H}$ delocalization energy associated with the C−H···O hydrogen bond with the CH_3 group on the P atom was calculated to be 0.7 kcal/mol, by using the natural bond orbital (NBO) population analysis implemented in the Gaussian03 program. Table 1 summarizes the Gibbs free

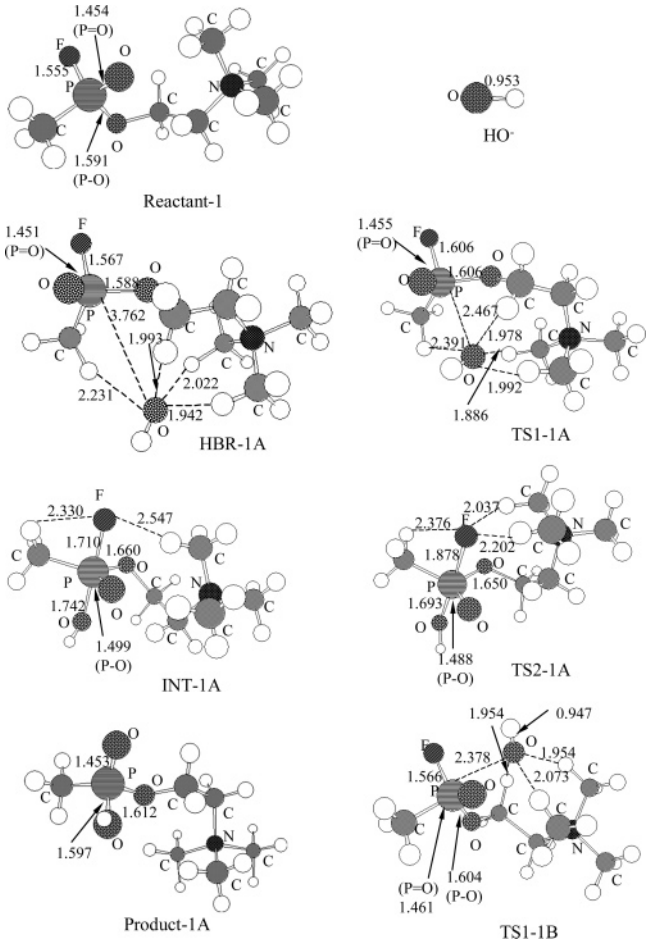

FIGURE 1. Geometries of reactants, hydrogen-bonded reactant complex, transition states, intermediate, and product optimized at the HF/6-31+G(d) level for the hydrolysis of 2-trimethylammonioethyl methylphosphonofluoridate, i.e. $(RO)CH_3P(O)F$ when $R = CH_2CH_2N^+(CH_3)_3$.

(36) Frisch, M. J.; Trucks, G. W.; Schlegel, H. B.; Scuseria, G. E.; Robb, M. A.; Cheeseman, J. R.; Montgomery, J. A., Jr.; Vreven, T.; Kudin, K. N.; Burant, J. C.; Millam, J. M.; Iyengar, S. S.; Tomasi, J.; Barone, V.; Mennucci, B.; Cossi, M.; Scalmani, G.; Rega, N.; Petersson, G. A.; Nakatsuji, H.; Hada, M.; Ehara, M.; Toyota, K.; Fukuda, R.; Hasegawa, J.; Ishida, M.; Nakajima, T.; Honda, Y.; Kitao, O.; Nakai, H.; Klene, M.; Li, X.; Knox, J. E.; Hratchian, H. P.; Cross, J. B.; Adamo, C.; Jaramillo, J.; Gomperts, R.; Stratmann, R. E.; Yazyev, O.; Austin, A. J.; Cammi, R.; Pomelli, C.; Ochterski, J. W.; Ayala, P. Y.; Morokuma, K.; Voth, G. A.; Salvador, P.; Dannenberg, J. J.; Zakrzewski, V. G.; Dapprich, S.; Daniels, A. D.; Strain, M. C.; Farkas, O.; Malick, D. K.; Rabuck, A. D.; Raghavachari, K.; Foresman, J. B.; Ortiz, J. V.; Cui, Q.; Baboul, A. G.; Clifford, S.; Cioslowski, J.; Stefanov, B. B.; Liu, G.; Liashenko, A.; Piskorz, P.; Komaromi, I.; Martin, R. L.; Fox, D. J.; Keith, T.; Al-Laham, M. A.; Peng, C. Y.; Nanayakkara, A.; Challacombe, M.; Gill, P. M. W.; Johnson, B.; Chen, W.; Wong, M. W.; Gonzalez, C.; Pople, J. A. *Gaussian 03*, Revision A.1; Gaussian, Inc.: Pittsburgh, PA, 2003.

(37) Zhan, C.-G.; Landry, D. W. *J. Phys. Chem. A* **2001**, *105*, 1296.

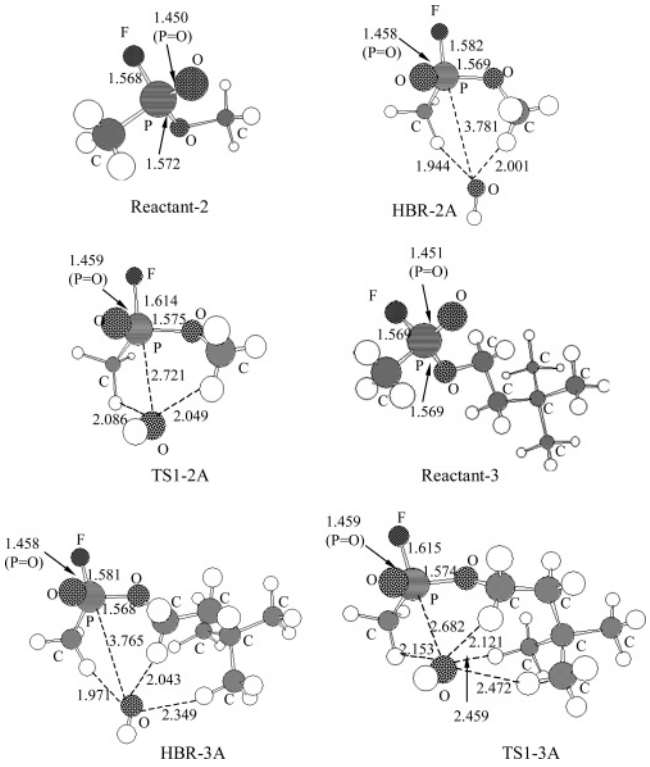

FIGURE 2. Geometries of reactants, hydrogen-bonded reactant complexes, and transition states optimized at the HF/6-31+G(d) level for the hydrolysis of $(RO)CH_3P(O)F$ when R = CH_3 and $CH_2CH_2C(CH_3)_3$.

energy barriers and enthalpy barriers calculated in both the gas phase and solution. The differences between the Gibbs free energy barriers and enthalpy barriers reflect the contributions from corresponding entropy changes. The data summarized in Table 1 reveal that both the entropy and solvation contributions to the free energy barriers are critical. Unless stated otherwise, the free energy barriers discussed below refer to those in aqueous solution.

The energetic results listed in Table 1 show that the highest free energy barrier is associated with the first step. So the first step is rate determining. As seen in Table 1, the free energy barriers calculated with three different basis sets are very close, suggesting that even the smallest basis set, 6-31+G(d), used in this study is sufficient for studying these reactions. With the largest basis set 6-311++G(d,p), the free energy barrier, 2.6 kcal/mol, calculated for the second step is negligible compared to the free energy barrier, 12.5 kcal/mol, calculated for the first step. The free energy barrier for the return of the intermediate INT-1A to TS1-1A was calculated to be 5.7 kcal/mol when the 6-311++G(d,p) basis set was used. So, we only calculated the first step of the hydrolysis associated with the reaction pathway B where the nucleophile OH^- attacks the P atom from a different orientation. The transition state corresponding to this reaction step is TS1-1B depicted in Figure 1. The optimized geometry of TS1-1B reveals three C−H···O hydrogen bonds between the hydroxide oxygen and the $CH_2CH_2N^+(CH_3)_3$ group. Compared to TS1-1A, the hydroxide oxygen in TS1-1B does not have a hydrogen bond with the CH_3 group on the P atom, but it still has three C−H···O hydrogen bonds with the $CH_2CH_2N^+(CH_3)_3$ group, as suggested by the optimized H···O distances in Figure 1. Based on the NBO analysis, the total $n_O \rightarrow \sigma^*_{C-H}$ delocalization energy associated with the three C−H···O hydrogen bonds with $CH_2CH_2N^+(CH_3)_3$ was calculated to be 34.1 kcal/mol, about 3.5 kcal/mol larger than that in TS1-1A. However, the calculated free energy barrier, 23.3 kcal/mol, associated with TS1-1B is 10.7 kcal/mol higher than that associated with TS1-1A. These energetic results suggest that pathway A is dominant for the alkaline hydrolysis of 2-trimethylammonioethyl methylphosphonofluoridate in aqueous solution.

We compared the calculated free energy barriers with available experimental kinetic data. For alkaline hydrolysis of 2-trimethylammonioethyl methylphosphonofluoridate in aqueous solution, the rate constant was measured to be 935 M^{-1} s^{-1} at T = 298.15 K.[2] This experimental rate constant gives an activation free energy of 13.4 kcal/mol according to the conventional transition state theory (CTST),[38] i.e.

$$k = (k_B T/h) \exp(-\Delta G/k_B T) \qquad (1)$$

where k_B is the Boltzmann constant, T is the absolute temperature, h is Planck's constant, and ΔG is the activation free energy. Our free energy barrier, 12.5 kcal/mol, calculated for the dominant reaction pathway is close to this experimentally derived activation free energy, 13.4 kcal/mol.

Alkaline Hydrolysis of Other Methylphosphonofluoridates. To better understand the substituent shifts of the free energy barrier for alkaline hydrolysis of methylphosphonofluoridate, $(RO)CH_3P(O)F$, we also examined the first step of the reaction pathway A for the hydrolysis of other methylphosphonofluoridates with R = CH_3, $CH_2CH_2C(CH_3)_3$, $CH_2CH_2CH(CH_3)_2$, $CH(CH_3)$-$CH_2N^+(CH_3)_3$, and $CH(CH_3)CH_2N(CH_3)_2$. The geometries optimized for the reactants and transition states are depicted in Figures 2 and 3. The calculated free energy barriers are given in Table 1. The optimized geometries of TS1-2A to TS1-6A in Figures 2 and 3 are similar to that of TS1-1A in Figure 1 in terms of the relative positions of the P, F, and HO^-. In particular, four C−H···O hydrogen bonds similar to those found in the TS1-1A geometry can also be found in the TS1-3A geometry. Three C−H···O hydrogen bonds with the $CH_2CH_2C(CH_3)_3$ group in TS1-3A are weaker than those with the CH_2-$CH_2N^+(CH_3)_3$ group in TS1-1A, whereas the C−H···O hydrogen bond with the CH_3 group on the P atom in TS1-3A is stronger than that in TS1-1A. In TS1-2A, the hydroxide oxygen only has two C−H···O hydrogen bonds with two CH_3 groups, but the optimized H···O distances in TS1-2A are all shorter than those in TS1-3A. Based on the NBO analysis, the total $n_O \rightarrow \sigma^*_{C-H}$ delocalization energy associated with the three C−H···O hydrogen bonds with $CH_2CH_2C(CH_3)_3$ was calculated to be 14.2 kcal/mol, whereas the $n_O \rightarrow \sigma^*_{C-H}$ delocalization energy associated with the C−H···O hydrogen bond with the CH_3 group on the P atom was calculated to be 6.2 kcal/mol. The total $n_O \rightarrow \sigma^*_{C-H}$ delocalization energy associated with all of the C−H···O hydrogen bonds in TS1-3A is 20.4

(38) Alvarez-Idaboy, J. R.; Galano, A.; Bravo-Pérez, G.; Ruíz, M. E. *J. Am. Chem. Soc.* **2001**, *123*, 8387.

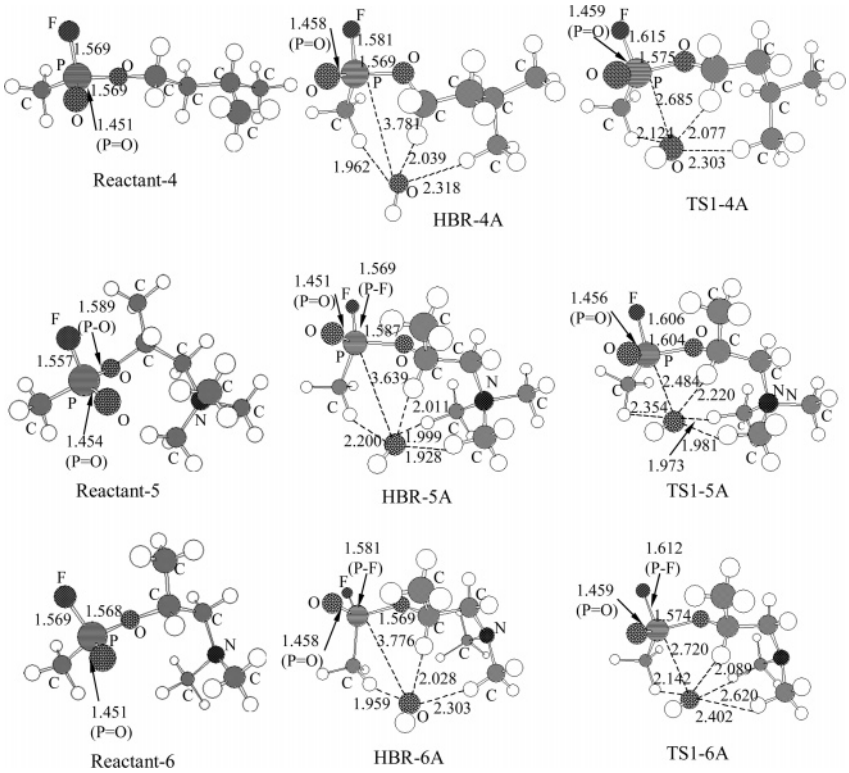

FIGURE 3. Geometries of reactants, hydrogen-bonded reactant complexes, and transition states optimized at the HF/6-31+G(d) level for the hydrolysis of $(RO)CH_3P(O)F$ when R = $CH_2CH_2CH(CH_3)_2$, $CH(CH_3)CH_2N^+(CH_3)_3$, and $CH(CH_3)CH_2N(CH_3)_2$.

kcal/mol, which is about 10.9 kcal/mol smaller than that of 31.3 kcal/mol in TS1-1A. The calculated free energy barriers associated with TS1-2A to TS1-3A are listed in Table 1. The calculated free energy barrier, 15.5 kcal/mol, associated with TS1-2A is close to the activation free energy, 14.7 kcal/mol, derived from the experimental rate constant, 106 M^{-1} s^{-1}, reported for the alkaline hydrolysis of $(CH_3O)CH_3P(O)F$ at T = 298.15 K.[2] The calculated free energy barrier, 13.4 kcal/mol, associated with TS1-5A is also close to the activation free energy, 13.9 kcal/mol, derived from the experimental rate constant, 381 M^{-1} s^{-1}, reported for the alkaline hydrolysis of $(RO)CH_3P(O)F$ when R = $CH(CH_3)CH_2N^+(CH_3)_3$ at T = 298.15 K.[2]

Electrostatic and Steric Effects. The aforementioned first-principles electronic structure calculations predict the free energy barrier for the alkaline hydrolysis of phosphonofluoridate $(RO)CH_3P(O)F$ to be 15.5 kcal/mol when R = CH_3, 17.9 kcal/mol when R = $CH_2CH_2C(CH_3)_3$, and 12.5 kcal/mol when R = $CH_2CH_2N^+(CH_3)_3$. The good agreement of the calculated free energy barriers with available experimentally derived activation free energies, 14.7 kcal/mol when R = CH_3, 13.4 kcal/mol when R = $CH_2CH_2N^+(CH_3)_3$, and 13.9 kcal/mol when R = $CH(CH_3)CH_2N^+(CH_3)_3$, suggest that the predicted free energy barriers are reliable. Hence, it is meaningful to discuss substituent shifts of the free energy barrier for the $(RO)CH_3P(O)F$ hydrolysis based on the predicted free energy barriers summarized in Table 1. Both CH_3 and $CH_2CH_2C(CH_3)_3$ are neutral functional groups. Compared to CH_3, $CH_2CH_2C(CH_3)_3$ has a larger bulk size and may have a significant effect of steric hindering to the hydroxide attacking at the P atom. As a result, the free energy barrier calculated with R = $CH_2CH_2C(CH_3)_3$ is 2.4 kcal/mol higher than that calculated with R = CH_3. The bulk size of $CH_2CH_2N^+(CH_3)_3$ is roughly the same as that of $CH_2CH_2C(CH_3)_3$. So, the steric effects of these two functional groups are roughly equivalent. The primary difference is that $CH_2CH_2N^+(CH_3)_3$ is positively charged, whereas $CH_2CH_2C(CH_3)_3$ is neutral. The positively charged functional group will have a strong electrostatic attraction to the attacking hydroxide anion and, therefore, the three C−H···O hydrogen bonds of the hydroxide oxygen with $CH_2CH_2N^+(CH_3)_3$ in TS1-1A are much stronger than the corresponding C−H···O hydrogen bonds with $CH_2CH_2C(CH_3)_3$ in TS1-3A. Because of the additional electrostatic attraction with $CH_2CH_2N^+(CH_3)_3$ in TS1-1A, the free energy barrier calculated with R = $CH_2CH_2N^+(CH_3)_3$ is 5.4 kcal/mol lower than that calculated with R = $CH_2CH_2C(CH_3)_3$.

The change of the substituent R in $(RO)CH_3P(O)F$ from CH_3 to $CH_2CH_2N^+(CH_3)_3$ is associated with both the steric and electrostatic effects on the free energy barrier. These two effects are expected to change the free energy barrier in two opposite directions. The substituent shift of the free energy barrier for the $(RO)CH_3P(O)F$ hydrolysis from R = CH_3 to $CH_2CH_2N^+(CH_3)_3$ due to the steric effect may be estimated to be the free energy barrier shift (2.4 kcal/mol) from R = CH_3 to $CH_2CH_2C(CH_3)_3$, whereas the free energy barrier shift due to the electrostatic effect may be estimated to be the free energy barrier shift (−5.4 kcal/mol) from R = $CH_2CH_2C(CH_3)_3$ to $CH_2CH_2N^+(CH_3)_3$. Therefore, the overall substituent shift of the calculated free energy barrier for the $(RO)CH_3P(O)F$ hydrolysis from R = CH_3 to $CH_2CH_2N^+(CH_3)_3$ is 2.4 + (−5.4) = −3.0 kcal/mol. The electrostatic effect dominates the substituent shift from R = CH_3 to $CH_2CH_2N^+(CH_3)_3$. This explains

TABLE 1. Calculated Gibbs Free Energy Barriers (ΔG) and Enthalpy Barriers (ΔH) in kcal/mol for the Alkaline Hydrolysis of Phosphonofluoridate (RO)CH_3P(O)F in Aqueous Solution When T = 298.15 K and P = 1 atm in Comparison with Available Experimental Data[a]

method[b]				MP2/BS1	MP2/BS2	MP2/BS3	expt[e]
R = $CH_2CH_2N^+(CH_3)_3$	path A[c]	step 1	ΔG	12.5	12.5	12.5	13.4
				(3.4)	(3.7)	(4.1)	
			ΔH	2.9	2.9	2.9	
				(1.6)	(1.8)	(2.2)	
		step 2	ΔG	3.1	3.1	2.6	
				(3.4)	(3.3)	(2.8)	
			ΔH	1.8	1.8	1.3	
				(2.1)	(2.0)	(1.5)	
	path B[d]	step 1	ΔG	23.4	23.3	23.3	
				(7.8)	(8.2)	(8.3)	
			ΔH	13.3	13.2	13.2	
				(3.9)	(4.3)	(4.4)	
R = CH_3	path A[c]	step 1	ΔG	15.4	15.2	15.5	14.7
				(3.8)	(3.9)	(4.6)	
			ΔH	7.0	6.7	7.1	
				(2.1)	(2.2)	(2.9)	
R = $CH_2CH_2C(CH_3)_3$	path A[c]	step 1	ΔG	17.9	17.7	17.9	
				(3.4)	(3.7)	(4.2)	
			ΔH	7.8	7.6	7.8	
				(1.4)	(1.6)	(2.1)	
R = $CH_2CH_2CH(CH_3)_2$	path A[c]	step 1	ΔG	16.4	16.3	16.5	
				(3.6)	(4.0)	(4.5)	
			ΔH	6.6	6.5	6.7	
				(1.8)	(2.1)	(2.6)	
R = $CH(CH_3)CH_2N^+(CH_3)_3$	path A[c]	step 1	ΔG	13.2	13.4	13.4	13.9
				(2.1)	(2.4)	(2.9)	
			ΔH	3.6	3.7	3.7	
				(0.4)	(0.8)	(1.2)	
R = $CH(CH_3)CH_2N(CH_3)_2$	path A[c]	step 1	ΔG	18.7	18.6	18.7	
				(2.6)	(3.0)	(3.5)	
			ΔH	8.8	8.7	8.9	
				(0.7)	(1.1)	(1.6)	

[a] Numbers in parentheses refer to the corresponding ΔG or ΔH values calculated for the reactions in the gas phase. [b] Method used in the gas-phase energy calculations. The basis sets BS1, BS2, and BS3 used in the MP2 energy calculations refer to 6-31+G(d), 6-31++G(d,p), and 6-311++G(d,p), respectively. Zero-point vibration and thermal corrections were performed at the HF/6-31+G(d) level. Solvent shifts were determined from the SVPE calculations at the HF/6-31+G(d) level. See text for the detailed methods. [c] Pathway A refers to the reaction pathway where the attacking nucleophile OH^- and the leaving group F^- are positioned on opposite sides of the plane formed by the three remaining atoms attached to the phosphorus. [d] Pathway B refers to the reaction pathway where the attacking nucleophile OH^- and the leaving group F^- are not on opposite sides of the plane formed by the three remaining atoms attached to the phosphorus. [e] Gibbs free energy barriers derived from the experimental rate constants (measured in water) at T = 298.15 K, 935 M^{-1} s^{-1} when R = $CH_2CH_2N^+(CH_3)_3$, 381 M^{-1} s^{-1} when R = $CH(CH_3)CH_2N^+(CH_3)_3$, and 106 M^{-1} s^{-1} when R = CH_3 (ref 2), based on the conventional transition state theory (ref 38).

why the alkaline hydrolysis of (RO)CH_3P(O)F with R = $CH_2CH_2N^+(CH_3)_3$ is significantly faster than that with R = CH_3.

The electrostatic and steric effects can also explain the relative magnitudes of the free energy barriers calculated for the (RO)CH_3P(O)F hydrolysis when R = $CH_2CH_2CH(CH_3)_2$, $CH(CH_3)CH_2N^+(CH_3)_3$, and $CH(CH_3)CH_2N(CH_3)_2$. When the size of R increases from $CH_2CH_2N^+(CH_3)_3$ to $CH(CH_3)CH_2N^+(CH_3)_3$, the calculated free energy barrier increases from 12.5 to 13.4 kcal/mol, whereas the experimentally derived activation free energy increases from 13.4 to 13.9 kcal/mol. The calculated free energy barrier for the (RO)CH_3P(O)F hydrolysis with R = $CH_2CH_2CH(CH_3)_2$ is between those with R = CH_3 and $CH_2CH_2C(CH_3)_3$, because the size of $CH_2CH_2CH(CH_3)_2$ is between the sizes of CH_3 and $CH_2CH_2C(CH_3)_3$. In addition, the size of $CH(CH_3)CH_2N(CH_3)_2$ is close to that of $CH_2CH_2C(CH_3)_3$, but the position of a methyl group is different. The free energy barrier, 18.7 kcal/mol, calculated with R = $CH(CH_3)CH_2N(CH_3)_2$ is close to the barrier, 17.9 kcal/mol, calculated with R = $CH_2CH_2N^+(CH_3)_3$, suggesting that the steric effect of the neutral amine substituent is not dramatically different from that of the neutral alkyl R group.

In addition, the concept of the electrostatic effect in the transition states can also help to better understand why the reaction pathway A has a much lower free energy barrier than pathway B. The primary difference between TS1-1A and TS1-1B is associated with the orientations of groups F^- and CH_3 relative to the attacking nucleophile OH^-, as seen in Figure 1. For a given phosphonofluoridate, (RO)CH_3P(O)F, both the attacking nucleophile OH^- and leaving F^- in the transition state have large amounts of negative atomic charge. For example, based on the NBO population analysis, the net atomic charge on group F^- is −0.665, whereas the net atomic charge on group CH_3 is −0.278, in TS1-1A. There is a strong electrostatic repulsion between the attacking and leaving groups in a transition state structure. The electrostatic repulsion destabilizes the transition state and, therefore, increases the free energy barrier. The electrostatic repulsion can be minimized when the OH^- and F^- are positioned on opposite sides of the plane

formed by the three remaining atoms attached to the P atom in pathway A. This qualitatively explains why the calculated free energy barrier associated with TS1-1A is lower than that associated with TS1-1B by 10.7 kcal/mol. Recent computational studies[32,33] indicated that the dominant reaction pathway for alkaline hydrolysis of phosphodiesters is a one-step process where the attacking and leaving groups are also positioned on opposite sides of the plane formed by the three remaining atoms attached to the P atom in the transition state. This can also be attributed to the effect of the electrostatic repulsion between the negative charges on attacking and leaving groups in the transition state, in light of the current analysis of the electrostatic effect.

Further, the concept of the electrostatic effect in the transition states can also be extended to explain why the rate constants for the alkaline hydrolysis of phosphodiesters, such as adenosine 3′,5′-phosphate (cAMP), dimethyl phosphate (DMP), and trimethylene phosphate (TMP),[32,33] are generally smaller than those for the alkaline hydrolysis of the aforementioned phosphonofluoridates and related phosphotriesters.[17] In contrast to the aforementioned neutral or cationic phosphonofluoridates and related phosphotriesters, the phosphodiesters primarily exist in the dissociated structural forms as anions in aqueous solution due to their small pK_a values. The strong electrostatic repulsion between the phosphate anion and OH^- destabilizes the transition state and, therefore, increases the free energy barrier. The experimentally estimated free energy barriers, ~29, ~32, and ~32 kcal/mol, for the alkaline hydrolysis of cAMP, DMP, and TMP, respectively,[33] are all significantly higher than those for the phosphonofluoridates and related phosphotriesters mentioned above. All of these results suggest that for the alkaline hydrolysis of phosphodiesters, phosphotriesters, and their structural variants, their electrostatic interactions with the attacking nucleophile OH^- favor the following order of free energy barriers:

$$\Delta G(M^+ + OH^-) < \Delta G(M^0 + OH^-) < \Delta G(M^- + OH^-) \quad (2)$$

in which M^+, M^0, and M^- represent the cationic, neutral, and anionic molecules, respectively.

Conclusion

First-principles electronic structure calculations were performed to study reaction pathways and free energy barriers for alkaline hydrolysis of the insecticide 2-trimethylammonioethyl methylphosphonofluoridate and related phosphonofluoridates, $(RO)CH_3P(O)F$, in aqueous solution. The calculated results indicate that the dominant reaction pathway for the alkaline hydrolysis is associated with a transition state in which the attacking nucleophile OH^- and the leaving group F^- are positioned on opposite sides of the plane formed by the three remaining atoms attached to the P atom in order to minimize the electrostatic repulsion between these two groups. The free energy barriers calculated for the rate-determining step of the dominant pathway are 12.5 kcal/mol when R = $CH_2CH_2N^+(CH_3)_3$, 15.5 kcal/mol when R = CH_3, 17.9 kcal/mol when R = $CH_2CH_2C(CH_3)_3$, 16.5 kcal/mol when R = $CH_2CH_2CH(CH_3)_2$, 13.4 kcal/mol when R = $CH(CH_3)CH_2N^+(CH_3)_3$, and 18.7 kcal/mol when R = $CH(CH_3)CH_2N(CH_3)_2$. The free energy barriers are in good agreement with available experimentally derived activation free energies, i.e., 14.7 kcal/mol when R = CH_3, 13.4 kcal/mol when R = $CH_2CH_2N^+(CH_3)_3$, and 13.9 when R = $CH(CH_3)CH_2N^+(CH_3)_3$.

The calculated results indicate that both the steric and electrostatic effects can significantly affect the free energy barrier for the alkaline hydrolysis of $(RO)CH_3P(O)F$. The change of the substituent R in $(RO)CH_3P(O)F$ from CH_3 to $CH_2CH_2N^+(CH_3)_3$ is associated with both the steric and electrostatic effects on the free energy barrier. These two effects affect the free energy barrier in two opposite directions. The substituent shift of the free energy barrier for the $(RO)CH_3P(O)F$ hydrolysis from R = CH_3 to $CH_2CH_2N^+(CH_3)_3$ due to the steric effect was estimated to be the free energy barrier shift, 2.4 kcal/mol, from R = CH_3 to $CH_2CH_2C(CH_3)_3$, whereas the free energy barrier shift due to the electrostatic effect was estimated to be the free energy barrier shift, −5.4 kcal/mol, from R = $CH_2CH_2C(CH_3)_3$ to $CH_2CH_2N^+(CH_3)_3$. So, the electrostatic effect dominates the substituent shift and the overall substituent shift from R = CH_3 to $CH_2CH_2N^+(CH_3)_3$ decreases the calculated free energy barrier for the $(RO)CH_3P(O)F$ hydrolysis, which is qualitatively consistent with the reported experimental data. This helps to better understand why the alkaline hydrolysis of $(RO)CH_3P(O)F$ with R = $CH_2CH_2N^+(CH_3)_3$ and $CH(CH_3)CH_2N^+(CH_3)_3$ is significantly faster than that with R = CH_3.

It has been suggested that the net charge of the molecule (M) being hydrolyzed is a prominent factor affecting the free energy barrier (ΔG) for the alkaline hydrolysis of phosphodiesters, phosphonofluoridates, and related organophosphorus compounds. The electrostatic interactions between the attacking nucleophile OH^- and the molecule being hydrolyzed favor such an order: $\Delta G(M^+ + OH^-) < \Delta G(M^0 + OH^-) < \Delta G(M^- + OH^-)$, where M^+, M^0, and M^- represent the cationic, neutral, and anionic molecules, respectively. This helps to understand why the rate constants for the alkaline hydrolysis of phosphodiesters, such as intramolecular second messenger adenosine 3′,5′-phosphate (cAMP), are generally smaller than those for the alkaline hydrolysis of the aforementioned phosphonofluoridates and related phosphotriesters.

Acknowledgment. This research was supported in part by NIH grant R01DA013930 and the University of Kentucky Research Foundation. We also thank the Center for Computational Sciences at the University of Kentucky for the support in terms of supercomputing time on the Superdome supercomputer. Some computation was done using the EMSL Molecular Sciences Computing Facility under Grand Challenge grant GC3565 in the Pacific Northwest National Laboratory.

Supporting Information Available: Cartesian coordinates of the geometries optimized at the HF/6-31+G(d) level, along with their total energies and numbers of imaginary vibrational frequencies. This material is available free of charge via the Internet at http://pubs.acs.org.

JO0487597